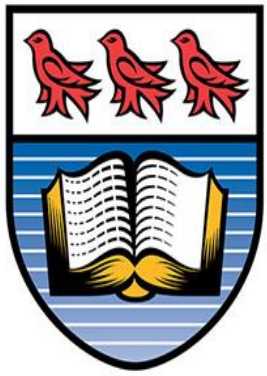

University of Victoria

UNIVERSITY OF VICTORIA

MECH 493 – Design of Thermo-Fluid Systems

Final Report

Due Date:
Monday, August 5th, 2024

Students:

Carmina Rocheleau	V01021553
Arturo Ramirez Aguilar	V00938676
Peter Kemp	V00966314
Jacob Gaucher	V00884749
Jayden Collins	V00863456

Summary

This report outlines the reverse engineering and optimization project undertaken on the Chefman Iceman Mini Fridge, with a focus on improving the thermal performance of two key components—the Peltier cooler's cold block and the heat sink. Computational Fluid Dynamics (CFD) tools were employed to create simulations of the mini fridge's hot side (the heat sink and fan) and the cold side (the cold block and insulated volume). Simulations of the hot side suggested modifying the heat sink to have an increased number of fins and triangular fin profile, instead of rectangular, would increase the COP by up to 53% with only a minor 9.9% increase in cost. Cold side simulations suggest increasing the surface area of the cold block would increase its efficiency at cooling the insulated section of the fridge.

Overall, this study underscored the advantages of CFD, which facilitated targeted modifications based on fluid flow dynamics rather than relying solely on traditional methods such as maximizing surface area. Future work should focus on conducting mesh convergence studies to validate simulation accuracy, experimenting with an optimized gyroid fin pattern featuring larger pores for enhanced heat dissipation, and undertaking a more comprehensive cost analysis to address overlooked factors such as labor and shipping costs. This project demonstrates the significant potential of CFD applications in driving substantial improvements in appliance design and efficiency, providing a robust framework for future enhancements.

Table of Contents

Table of Figures

1 Introduction

In this project, our primary objective was to reverse engineer and improve the thermal performance of the Chefman Iceman Mini Fridge, shown in Figure 1. With a specific focus on enhancing its coefficient of performance (COP) while maintaining a balance between performance improvements and additional costs.

Figure 1: Chefman Iceman Mini Fridge

The mini fridge utilizes a TEC1-12704 Peltier cooler, a thermoelectric device with a baseline COP of 0.125, as its primary cooling mechanism, as shown in Figure 2 below.

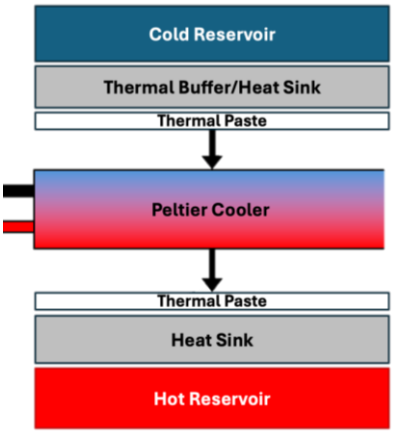

Figure 2: Chefman Iceman Mini Fridge Cooling System

Given the numerous potential areas for analysis within the mini fridge, we strategically limited the scope of our investigation to two key components: the cold side (Peltier cooler) and the hot side (heat sink).

The cold side of the system, where the cooling effect is directly applied, was analyzed using steady-state thermal simulations in SolidWorks. Our focus was on understanding the temperature distribution across the metal insert that comes into direct contact with the Peltier

cooler. By simulating various scenarios with different contact areas between the cooler and the metal insert, we aimed to identify how these variations could impact the overall temperature distribution and, consequently, the cooling efficiency of the fridge. The analysis revealed that optimizing the contact area could lead to a more uniform temperature distribution, which in turn could enhance the overall cooling performance. This insight is crucial for developing design modifications that could improve thermal conduction on the cold side, potentially leading to a higher COP.

On the hot side, we conducted a comprehensive conjugate heat transfer analysis using Simcenter Star-CCM+ to evaluate the performance of the heat sink attached to the Peltier cooler. The primary goal was to investigate how various design changes could improve the heat dissipation capabilities of the heat sink, thereby enhancing the overall efficiency of the cooling system. Our analysis explored several key factors, including modifications to the fin geometry, fin spacing, and the introduction of novel heat sink designs. By running multiple CFD simulations, we were able to assess the impact of these changes on the heat sink's ability to dissipate heat. The results highlighted that certain geometric modifications could significantly improve heat transfer, leading to better management of the thermal load on the Peltier cooler.

While the Chefman Iceman Mini Fridge contains numerous components that could potentially be optimized, our decision to focus on the cold and hot sides of the Peltier cooler allowed for a detailed and targeted analysis. The insights gained from the thermal and CFD simulations provided valuable guidance for design improvements that could enhance the fridge's COP without incurring excessive costs. Our work demonstrates that even with a constrained scope, meaningful performance enhancements can be achieved through careful analysis and strategic design modifications.

1.1 Mini Fridge Components

The disassembly of the Chefman Iceman Mini Fridge was the initial step in our project. It provided us with a clear understanding of its internal structure, enabling us to identify and analyze the critical components of its cooling system. During this process, we carefully dismantled the fridge to expose the key elements of the cooling system. The various components have been broken down into are listed in Table 1, and shown in Figure 3 below. Fasteners and other minor components have not been listed but are required to achieve the full assembly as shown in Figure 1 above.

Table 1: Mini Fridge Component List

Component #	Component Name	Component #	Component Name
1	Back Cover	**8**	Rubber Gasket
2	Foam Insulation	**9**	Heat Sink
3	Internal Shell	**10**	Metal Insert
4	Plastic Cover	**11**	Fan
5	Front Door	**12**	Circuit Board
6	Shelf	**13**	Wiring Connections
7	Peltier Cooler		

To help identify components in Figure 3 numbers and colors have been assigned to each.

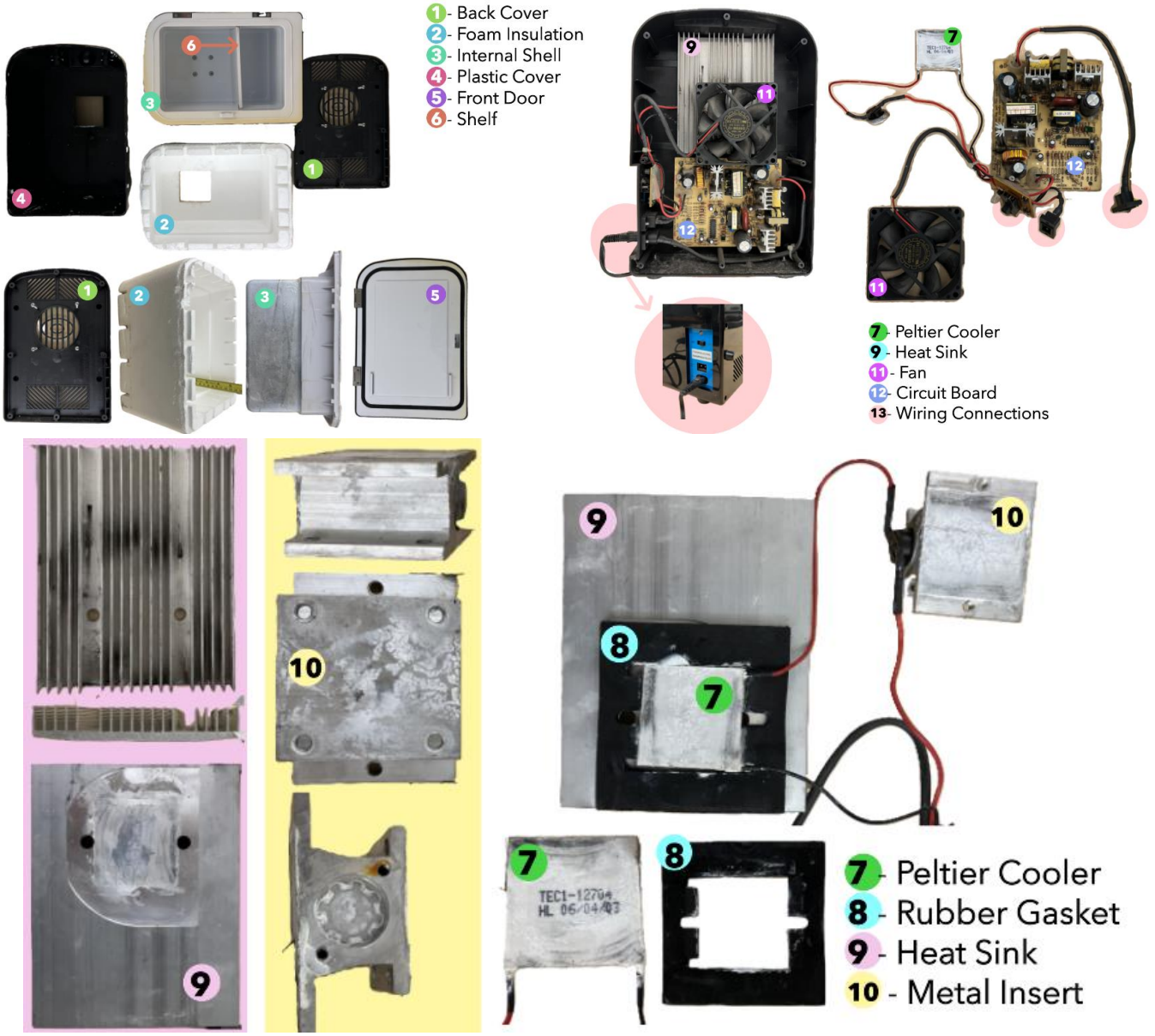

Figure 3: Mini Fridge Disassembled Component Breakdown

1.2 Goals of CFD Analyses

In both the hot side and cold side of the fridge, there are several components worthy of a CFD analysis. However, given the time and resource constraints of the project, scope was limited to a single component on each side. The CFD studies of each side were devised as follows:

- **Cold side**: investigated how changing the cold block dimensions impacts temperature gradients within the fridge's insulated volume
- **Hot side**: investigated how (a) changes to the hot side heat sink dimensions, and (b) different heat sink designs, impact thermal resistance and cost

2 Methodology

2.1 Cold Side

The cold side of the Peltier was analyzed using a steady-state SolidWorks simulation of the inside of the fridge. The temperature was averaged throughout the metal insert and the contact area to the Peltier was increased incrementally to measure its effect on the average temperature.

The cold side of the fridge is to be modelled and simulated in SolidWorks using its steady-state thermal analysis. A cross-section side view of the modelled components for this simulation are shown in Figure 4. A temperature condition is set on the Peltier cooler model with the temperature set at -8C. There is an ambient condition set on the air around the fridge set at 20C. Figure 4 shows how these conditions are set up.

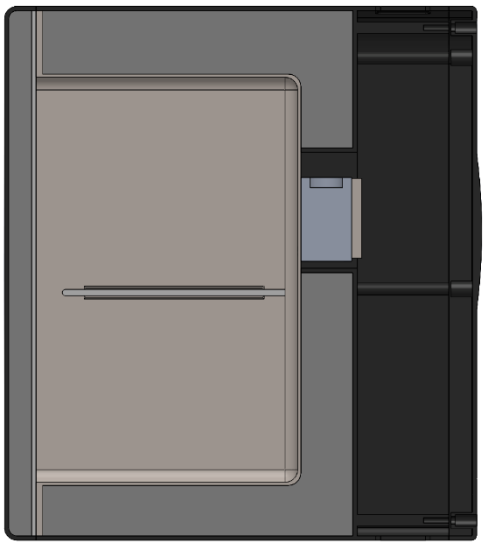

Figure 4: Cross-section of the cold side simulation setup.

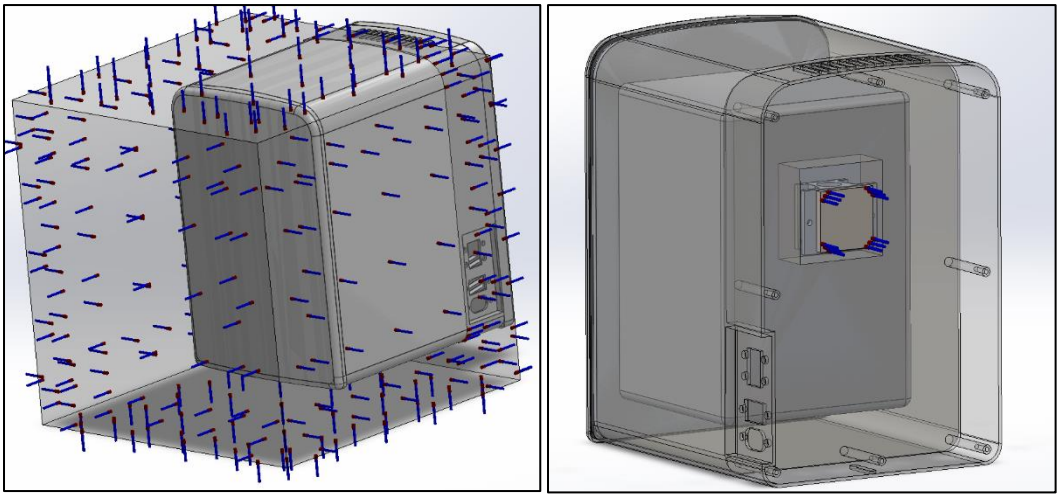

Figure 5: Set up of simulation temperatures.

The models were meshed using a maximum element size of 23.75mm and minimum element size of 1.19mm. The meshed part can be seen in Figure 6. Convergence analysis was not done for this simulation. This was an oversight in the simulation and if further simulations are to be done with this project convergence analysis will be done.

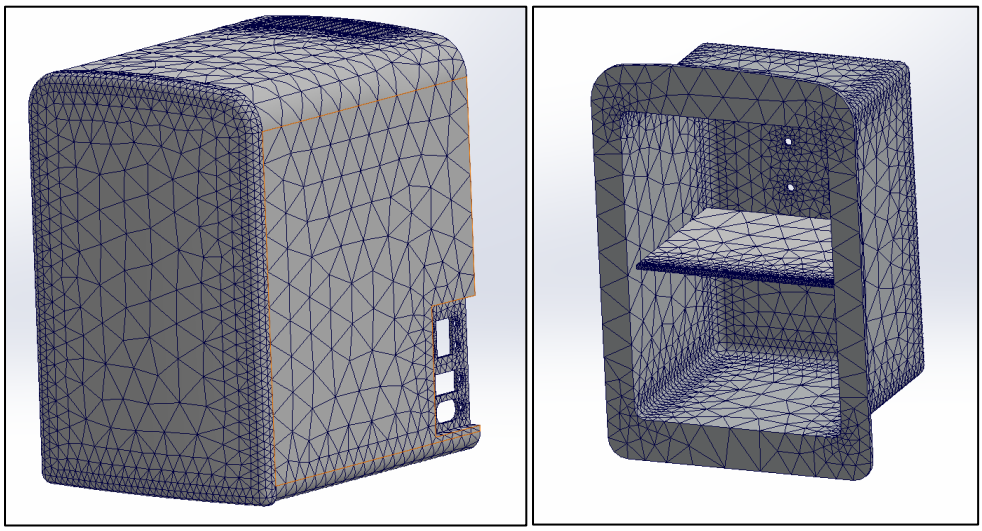

Figure 6: SolidWorks simulation mesh setup.

2.2 Hot Side

2.2.1 Fin Equation Analysis

Analysis of the hot side focused on the heat sink that is mounted to the hot side of the Peltier cooler. As a preliminary analysis, the fin equation was used to determine the best-performing fin shape that maximized heat flux across the heat sink. In this study, a MATLAB script was written to model the system parameters: number of fins; fin length, width, and thickness; fin spacing; base plate thickness; Peltier and environmental temperatures; and heat transfer coefficients.

Assumptions in the analysis included one-dimensional heat conduction in the fins, steady-state conditions, and uniform convective heat transfer coefficient. The analysis was performed using the same parameters as the original heat sink, where only the fin shape was changed. The results of this study, shown in Figure 15, demonstrate the need for more detailed analysis using CFD to find ideal fin parameters.

2.2.2 CFD Analysis

In this study, conjugate heat transfer across the heat sink is simulated using Simcenter Star-CCM+. The first half of the analysis measured how the heat sink performance changes as various parameters — depicted in Figure 7 — are modified. Table 2: Heat Sink Parameters lists the parameters of the existing heat sink. Note the existing array of 18 fins has two gaps where fins are missing. As the number of fins are changed in simulations, these gaps are ignored, and fins are spaced evenly across the width of the heat sink.

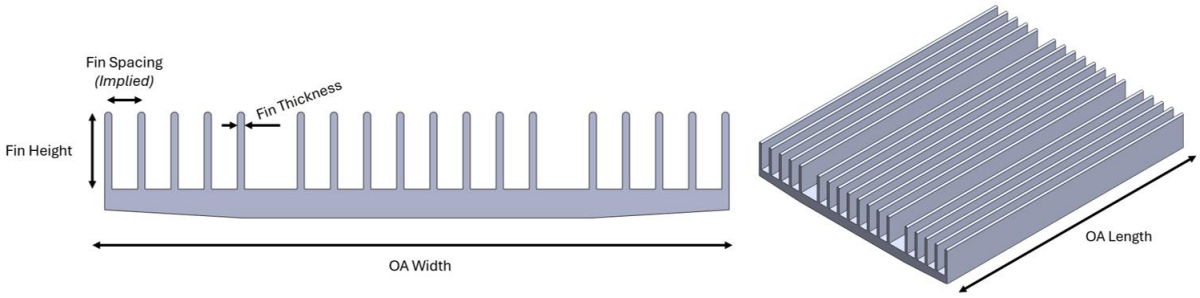

Figure 7: Heat Sink and Relevant Parameters

Table 2: Heat Sink Parameters

N Fins	Fin Height	Fin Thickness	OA Width	OA Length
18	12.6 mm	1.2 mm	102.4 mm	128.8 mm

The second part of this study involved testing completely different heat sink designs. Instead of varying the parameters, the authors modelled novel heat sinks that fit into the same envelope as the existing design. Figure 8 shows 3D models of the designs tested.

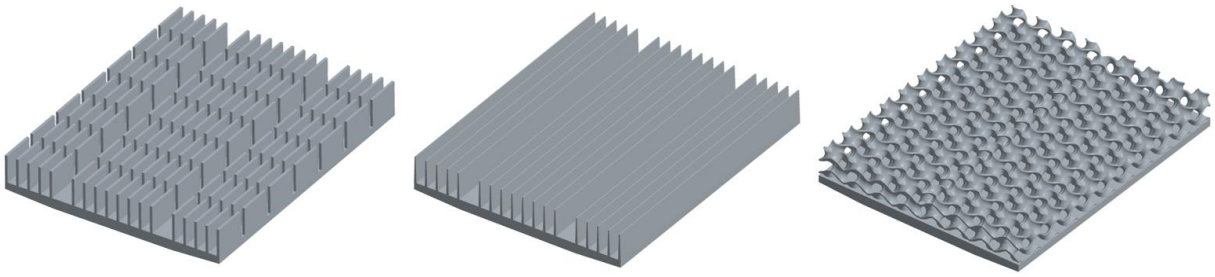

Figure 8: Tested 3D Models

2.2.2.1 Simulation Setup: Mesh and Boundary Conditions

Heat sinks were simulated in simplified benchtop conditions which are depicted in Figure 9. The heat sink is placed on a no-slip wall surrounded by a large fluid domain. The walls of the fluid domain are configured as pressure outlets at atmospheric pressure and 300K (26.9 °C). A 30 W of heat source is distributed across a 40 mm x 40 mm split surface on the bottom surface of the heat sink. To model the case fan that pushes air over the mini fridge's heat sink, a mass flow inlet is assigned to an 80 mm x 80 mm split surface at the top of the fluid domain. Disassembly of the mini fridge revealed a Yate Loon D80SM-12B fan, with a nominal airflow rate of 24 CFM [1]. Assuming the air is near room temperature with a density of approximately 1.2 kg/m^3 gives a mass flow rate of approximately:

$$\dot{m} = \dot{V} \times \rho = 24\ \text{CFM}\left(\frac{1\ \text{m}^3/\text{s}}{2118.87\ \text{CFM}}\right) \times 1.2\frac{\text{kg}}{\text{m}^3} = 0.0136\ \text{kg/s}$$

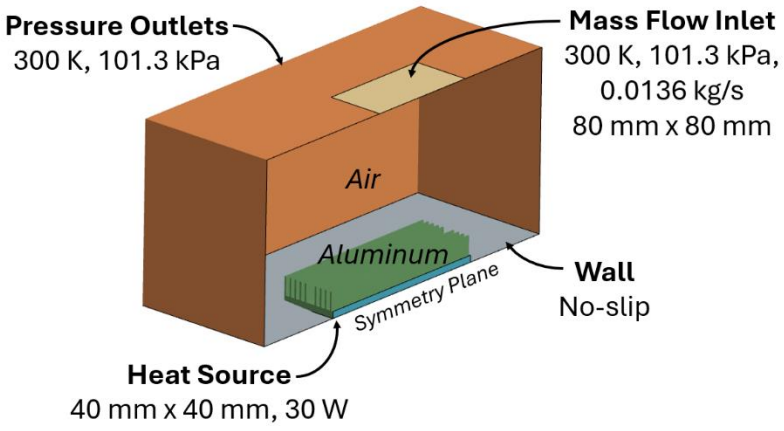

Figure 9: Heat Sinks Simulated Benchtop Conditions

The fluid domain was modelled as air and the heat sink as aluminum. Material and interface properties were left unchanged from the default values in Star-CCM+. To save computational resources, flow was approximated as symmetric about the center of the heat sink. Simulations were run using a steady-state, constant density assumptions with turbulent conditions. Gravity was directed towards the bottom wall. The K-Omega SST turbulence model was employed.

Two mesh types were used in the simulation. The heat sink region featured relatively simple geometry and was meshed using Star-CCM+'s highly efficient trimmed cell mesher. The fluid domain was meshed with polyhedral cells instead. Generally, aligning a structured mesh with the direction of flow can provide more accurate results than an unstructured mesh (e.g., a polyhedral mesh) [2]. However, creating such a mesh relies on knowing the direction of flow a priori, which was not the case in this study. To model the boundary layer, two prism layers were added to the air-fin interface and the air-wall interface. Figure 10 shows a cross section of the mesh around the heat sink and Table 3 lists important mesh parameters. Note that Star-CCM+ automatically repairs low-quality cells, meaning that some cells deviate from the size settings in Table 3.

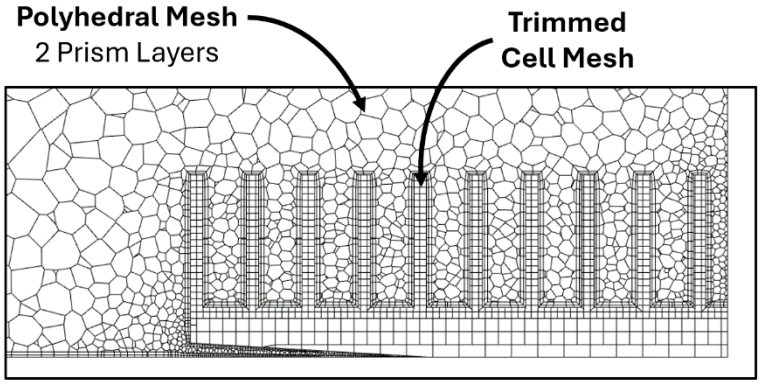

Figure 10: Cross Section Mesh Around Heat Sink

Table 3: Mesh Parameters

Region	Mesh Type	Base Size	Target Surface Size	Minimum Surface Size
Heat Sink	Trimmed Cell	5.0 mm	2.5 mm	0.5 mm
Fluid Domain	Polyhedral	1.0 cm	1.0 cm	2.5 mm

2.2.2.2 Cost Accounting

Any changes to the heat sink were analyzed in the context of additional costs. The existing heat sink is a simple aluminum extrusion. For any simple changes to the heat sink's cross-sectional geometry (i.e. the parameters in part of this study), differences in cost were assumed to be equal to the change in volume. In other words, an extruded heat sink that uses 10% more material than the existing design would cost 10% more to manufacture.

The second part of the study involved certain novel designs that were no longer pure aluminum extrusions. The split fin design would involve an additional machining step to cut the fins. The additional costs associated with machining an extruded heat sink were estimated using industry rules-of-thumb. Gabrian, a manufacturer of custom aluminum extrusions, claims aluminum

costs anywhere from $1,500 to $3,500 (USD) per metric ton, with an additional $200-$300 per metric ton if machining is required [3]. Therefore, assuming the price of aluminum is $C_{Mat} =$ $2,500 per ton and machining costs $C_{Mach} =$$300 per ton, this gives an overall price estimate of:

$$C_{Total}(\$CAD) = \text{Material} + \text{Machining} C_{Total}(\$CAD) = (V\rho_{al}C_{Mat} + V\rho_{al}C_{Mach}) \times (\text{Exchange Rate})$$
$$C_{Total}(\$CAD) = (V\rho_{al}C_{Mat} + V\rho_{al}C_{Mach}) \times (\text{Exchange Rate})$$
$$C_{Total}(\$CAD) = (V(0.0027)(2{,}500) + V(0.0027)(300)) \times (1.39)$$
$$\mathbf{C_{Total}(\$CAD) = 9.38V + 1.13V}$$

Where V is the volume of the heat sink (in cubic centimeters) and ρ_{al} is the density of aluminum (approximately 0.0027 kg/cm^3). Note the second term, $1.13V$, is zero for any designs where there is no machining required after the extrusion process. Of course, this simplified analysis neglects additional costs like labour and shipping, but accounting for these costs would involve a significantly more detailed analysis that was outside of the scope of this project.

The gyroid heat sink analyzed would probably only be manufacturable with additive methods. Therefore, the cost of the gyroid heat sink was estimated using instant an instant quoting tool, Xometry [4], for direct metal laser sintering. According to this tool, the cheapest quote had a unit cost of approximately $1004.42 CAD.

3 Results and Discussion

3.1 SolidWorks Simulation

For the SolidWorks simulation 7 different trials were simulated. First the current setup of the fridge was simulated to find the baseline numbers for the latter simulations with the larger cold block contact areas. The cold block and the dimension that is being optimized can be seen in Figure 11. The contact area for the cold was initially increased to 1.75 in by 1.75 in then each subsequent simulation increased the length and height by 0.5 in. Figure 12 shows the temperature gradient of the base simulation. For the purposes of comparing performance changes the average temperature of the inside surface is the data being taken from the simulation.

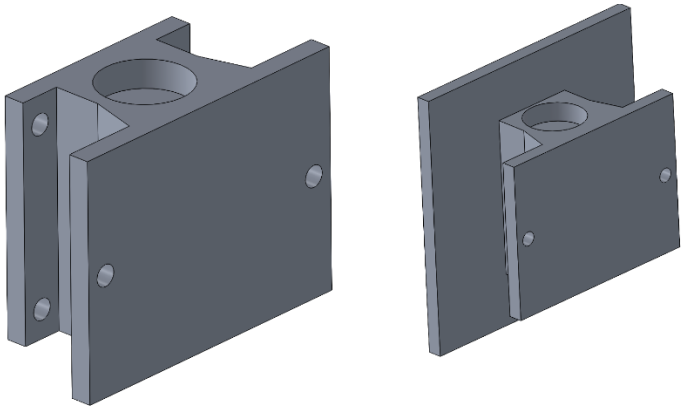

Figure 11: Original (left) and optimized (right) cold block.

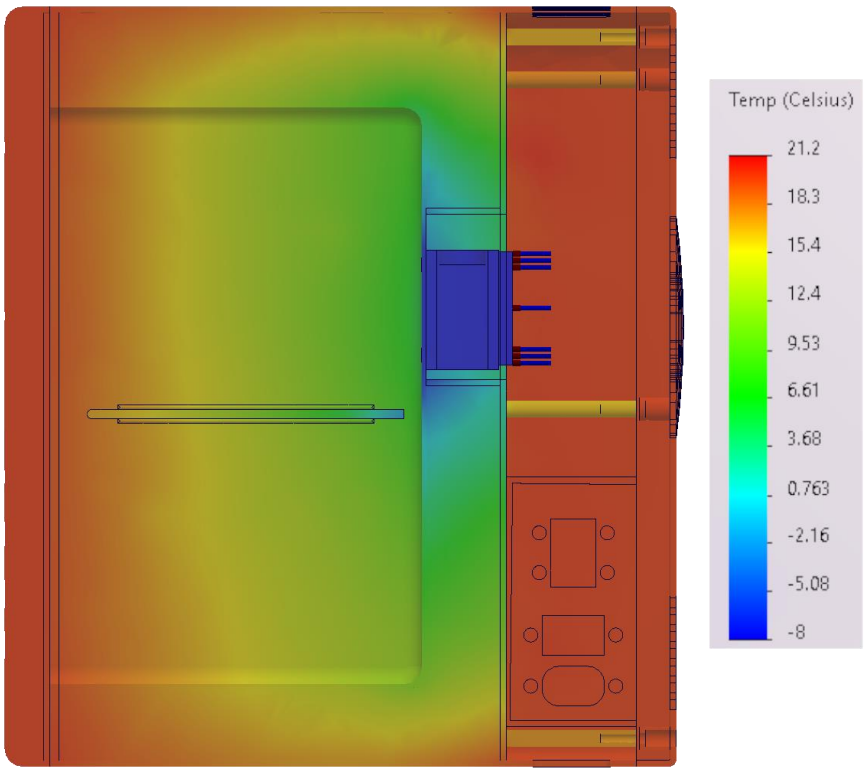

Figure 12: Base cold side temperature gradient

Each simulations results can be seen summarized in Table 4 and Figure 14Figure 14. Looking at each simulation with a larger contact area, the average temperature decreases. When looking at the change in temperature per unit area a maximum of 0.304 $[C/in^2]$ can be seen. This max happens when the 2.75 in by 2.75 in cold block is simulated. After this point the effectiveness of the heat transfer diminishes. This diminishing result may be from the decreased temperature through the system allowing for more heat gain. For better insight into this the heat gain through the exterior of the system should be analyzed.

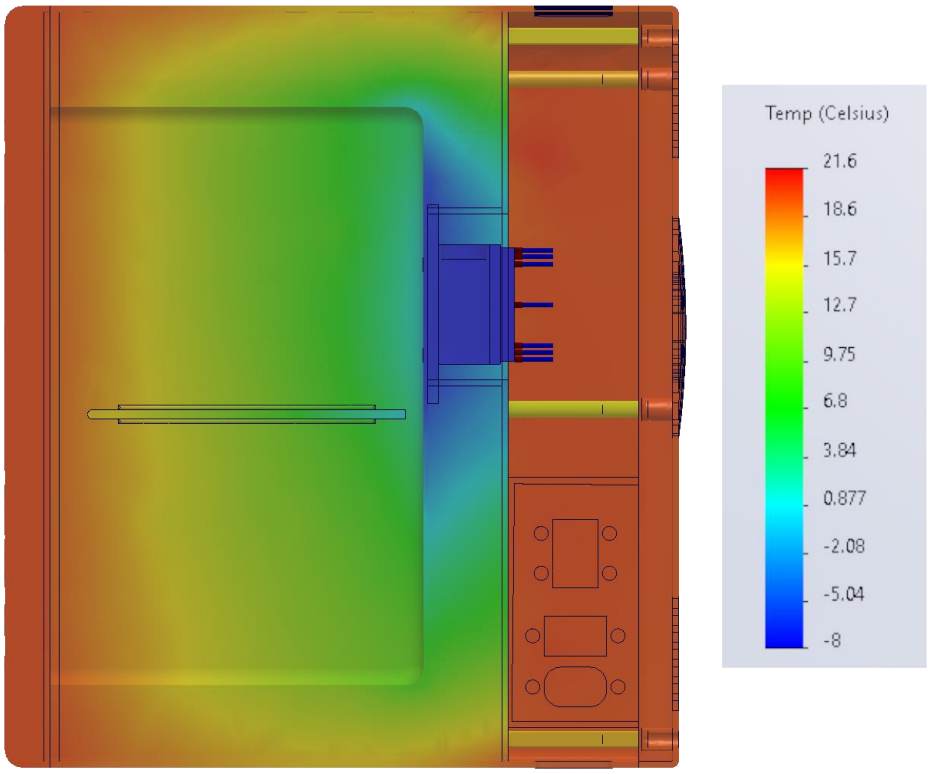

Figure 13: Simulation result from optimized contact area.

In Figure 13 an improvement of the temperature gradient can be seen where temperatures under 0C now take up most of the back wall of the fridge. The side walls also have an improved temperature gradient where the green and yellow colouring is extended more towards the front.

Future changes to this simulation will include measuring the heat gain into the system to gain insight on the maximum found with the 2.75in by 2.75 in cold block. The geometry of the cold block should also be looked at to see if changes to that will improve the cooling of the system.

Table 4: SolidWorks simulation results.

Size [in]	Area [in^2]	Avg Temp [C]	dT/Area [C/in^2]
Base	2.4734	10.9	-
1.75x175	3.0625	10.9	0.000
2.25x2.25	5.0625	9.49	0.279
2.75x2.75	7.5625	8.6	0.304
3.25x3.25	10.5625	8.01	0.274
3.75x3.75	14.0625	7.4	0.249
4.25x4.25	18.0625	6.74	0.230

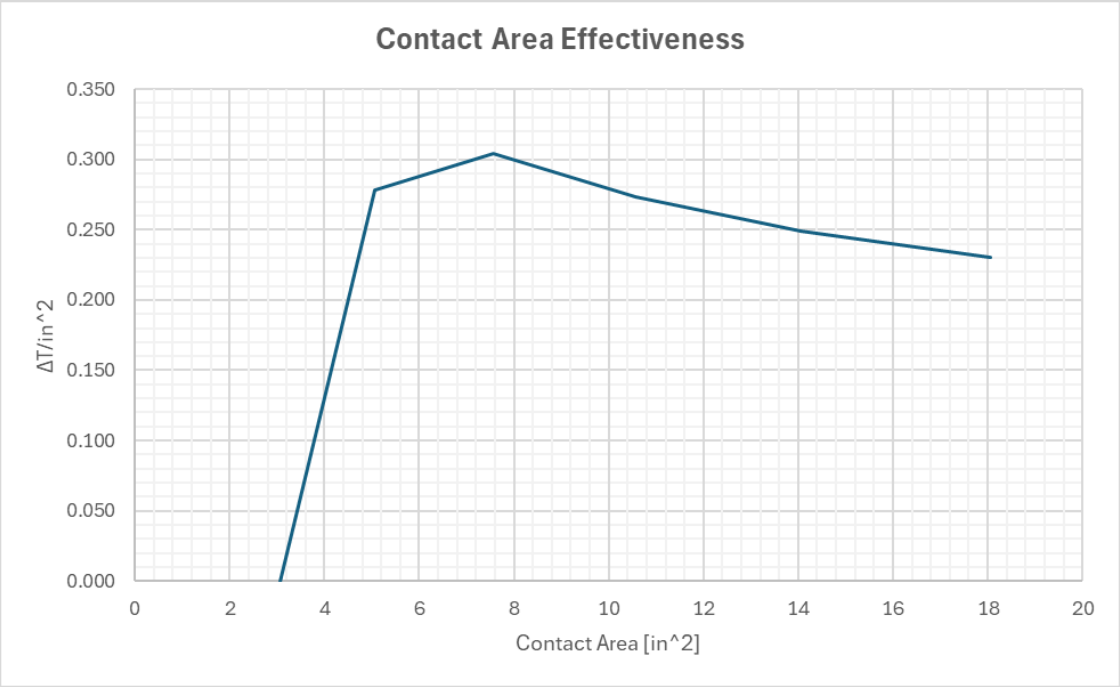

Figure 14: Graphed results of the SolidWorks simulation.

3.2 Hot Side

3.2.1 MATLAB Analysis

The fin equation was performed for each of the three basic fin shapes: straight, triangular, and parabolic. The input parameters are the same as those outlined in Trial 1 of Table 6, with only the fin shape being different between the simulations. Figure 15 shows the resulting heat flux across the three basic fin shapes. Although the parabolic fin shape yielded the greatest heat flux among them, the difference between the largest and smallest heat flux is only 0.7%. This small difference initially suggests that fin shape is not the major contributor to heat flux, and a parametric study with more detailed analysis is required to find the ideal parameters for maximizing heat flux.

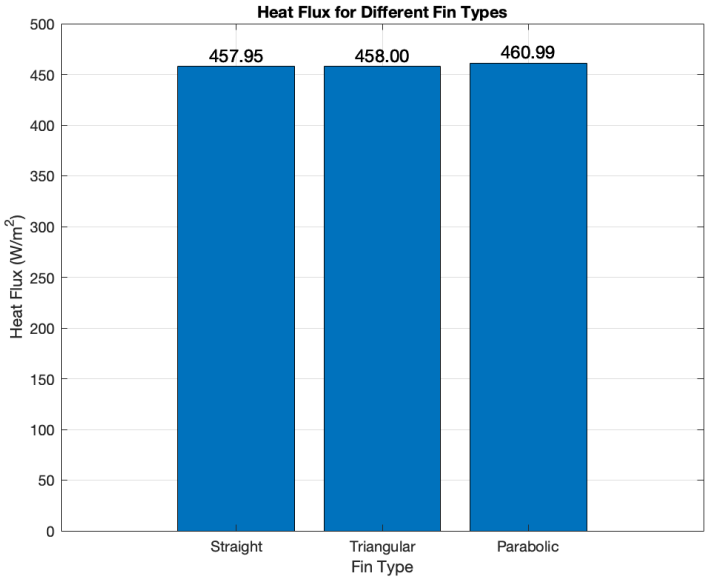

Figure 15: Heat Flux for Different Fin Types

3.2.2 Parametric Study

During each simulation, the average temperature of the heat sink over the heat source was monitored. This temperature is hereafter referred to as the "Peltier temperature." Simulations were deemed to have converged once the Peltier temperature plateaued at an approximately fixed value with further iterations. Figure 16 shows representative results from the simulation of the unmodified heat sink in the form of velocity streamlines, a velocity section, and a temperature section. Results of the parametric study are summarized in Table 5. This table also shows the thermal resistance of each heat sink, which is the difference between the ambient temperature and Peltier temperature, divided by heating power: $R = \Delta T/Q$. A lower thermal resistance corresponds to better thermal performance.

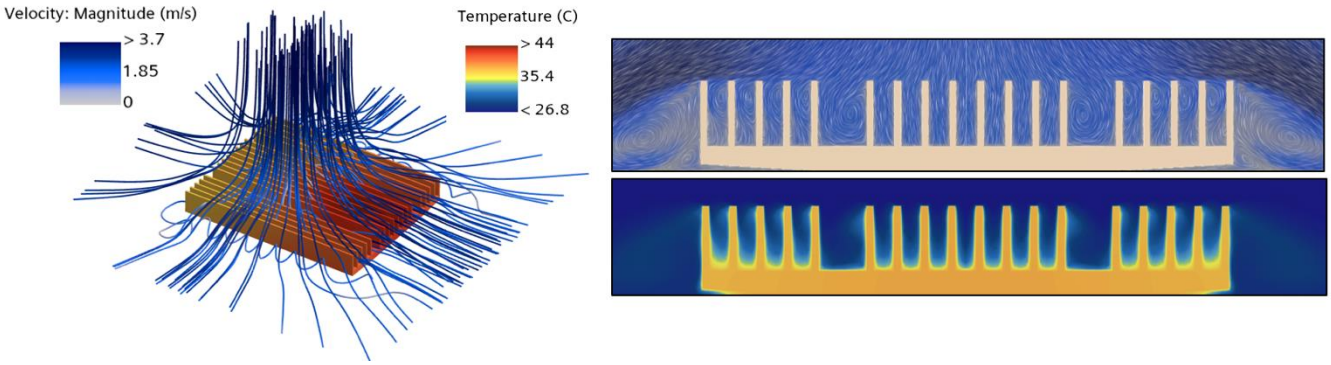

Figure 16: Simulation of Unmodified Heat Sink

Table 5: Results of the Parametric Study

Trial	Notes	N Fins	Fin Thickness (mm)	Fin Height (mm)	OA Width (mm)	OA Length (mm)	Fin Spacing (mm)	Surf-Avg Peltier Temp (°C)	Therm. Resist. (K/W)	% Change in Therm. Resist	Volume (cm^3)	% Change in Volume
1	Unmodified	18	1.19	12.61	102.37	128.77	5.95	43.5	0.553	--	93.4	--
2	Taller fins	18	1.19	**18**	102.37	128.77	5.95	40.2	0.443	-20%	108.2	15.9%
3	Shorter fins	18	1.19	**8**	102.37	128.77	5.95	49.1	0.740	34%	80.7	-13.6%
4	Thicker fins	18	**1.8**	12.61	102.37	128.77	5.92	43.4	0.550	-1%	111.2	19.1%
5	Thicker fins	18	**2.75**	12.61	102.37	128.77	5.86	44.2	0.577	4%	139.0	48.8%
6	Thinner fins	18	**1.0**	12.61	102.37	128.77	5.96	43.8	0.563	2%	87.8	-5.9%
7	Thinner fins	18	**0.5**	12.61	102.37	128.77	5.99	44.6	0.590	7%	73.2	-21.6%
8	Longer OA	18	1.19	12.61	102.37	**160**	5.95	42.8	0.530	-4%	116.0	24.3%
9	Shorter OA	18	1.19	12.61	102.37	**100**	5.95	45.9	0.633	14%	72.5	-22.3%
10	Wider OA	18	1.19	12.61	**150**	128.77	8.75	43.1	0.540	-2%	122.4	31.1%
11	Less wide OA	18	1.19	12.61	**80**	128.77	4.64	44.6	0.590	7%	79.7	-14.6%
12	No skipped fins	**20**	1.19	12.61	102.37	128.77	5.33	42.6	0.523	-5%	97.2	4.1%
13	More fins	**25**	1.19	12.61	102.37	128.77	4.22	41.1	0.473	-14%	106.9	14.5%
14	Less fins	**15**	1.19	12.61	102.37	128.77	7.23	45.7	0.627	13%	87.6	-6.2%
15	More fins	**32**	1.19	12.61	102.37	128.77	3.26	40.6	0.457	-17%	120.4	29.0%

To visualize key results, Figure 17 shows the Peltier temperature and volume plotted against the number of fins, fin height, and fin spacing. A few notable trends emerge from the results.

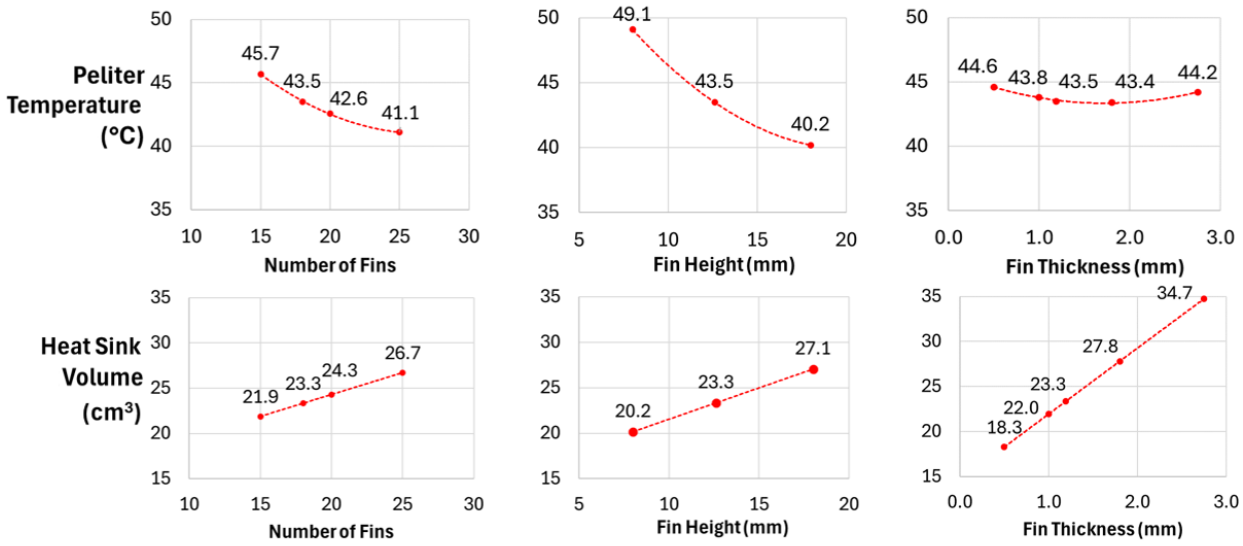

Figure 17: Peltier Temperature and Volume Plotted Against Various Conditions

Increasing the size of the heat sink, or the height of the fins, lowers the Peltier temperature at the cost of increasing the overall envelope and material requirements. This aligns with expectations, as adding more material generally increases the surface area available for convection. However, results suggest there are better ways to "spend" the additional material. For example, increasing the heat sink's overall length by 58 mm (Trial 8) only reduces the thermal resistance by 4%, but costs a 24% increase in volume. This contrasts with increasing the fin height to 18 mm (Trial 2),

which lowered the thermal resistance by 20%, yet costs only a 16% increase in volume. Results also suggest that the varying efficiency of additional material is not simply caused by changes surface area. Trials 2 and 8 increased surface area by 29% and 24% respectively, versus the existing design. In other words, increasing fin height is a more volume-efficient method of lowering Peltier temperature than increasing the outer dimensions. In any case, these changes still impact the overall envelope of the heat sink and implementing them would mean a partial redesign of the mini fridge's enclosure.

The fin thickness was already well-optimized, as evidenced by Figure 17 that shows the existing fin thickness is near a local minimum in Peltier temperature. The authors believe this local minimum represents the balance between two competing conditions. On one hand, thicker fins (and therefore smaller spaces between fins) restrict the amount of airflow between each fin thereby lowering the heat transfer coefficient in convection. On the other hand, making the fins thinner (and therefore increasing fin spacing) only improves heat transfer up to a certain point for two reasons. First, thinner fins lead to less overall surface area. And second, there is a practical limit to air much airflow is required to cool a single fin.

Adding more fins significantly decreases heat sink's thermal resistance, but returns are diminishing. This was an expected result as increasing the number of fins increases the heat sink's surface area which is directly proportional to convective heat transfer. The diminishing returns associated with additional fins also aligns with the previous discussion about fin spacing; as the number of fins increases, the fin spacing decreases, thereby limiting airflow between the fins. In the range of values tested, the heat transfer gained due to the additional surface area from extra fins outweighs the heat transfer lost due to decreased airflow from reduced spacing. However, the authors expect increasing the number of fins beyond a certain point would eventually increase the thermal resistance as the spacing between fins approaches zero.

3.2.3 Alternative Heat Sink Designs

This study also investigated the effect of replacing the existing heat sink with entirely new heat sink designs. The first two alternative designs involve relatively simple changes. In the first alternate design, fins were split by rectangular extruded cuts. Split fins are commonplace on many heat sinks and have been shown to increase thermal performance versus straight fins [5], but creating the cuts would require additional machining after extrusion. The second alternate design simply changed the cross-sectional geometry of each extruded fin from rectangular to triangular. The triangular fins retained the existing base thickness but tapered down to 0.5 mm at the fin tip.

To provide an interesting comparison, the authors devised the third alternate design by disregarding manufacturing costs and focusing solely on performance. This led to the creation of gyroid fins. Gyroids are triply periodic minimal surfaces with a high surface-to-volume ratio [6]. While manufacturing such structures been impractical historically, recent advances in metal additive manufacturing have made fabricating complex 3D structures possible, albeit with several limitations – notably cost. Following these advances, a research trend of designing heat exchangers and heat sinks that employ complex structures like gyroids has emerged [7]. The gyroid fins in this study were modelled as an array of gyroid unit cells that were two units tall, with a surface thickness of 0.75 mm, as shown in Figure 18. Like the other alternative designs, the outer envelope of the gyroid heat sink is identical to the existing heat sink. Finally, note the gyroid heat sink was modelled as symmetric in simulations despite the fact it is not. Symmetry was a necessary simplification as the computational requirements of simulating the full design were beyond what was available to the authors. Fins were meshed using an unstructured polyhedral mesh like the fluid domain.

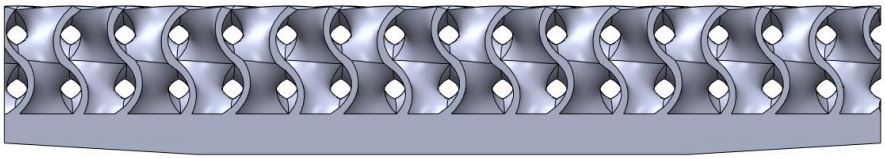

Figure 18: Gyroid Fins

The results of the alternative design simulations and the original design are summarized in Table 6. Like the previous simulations, the Peltier temperature, thermal resistance, and volume are listed for each design. Figure 19 shows the temperature distributions over each heat sink. A few notable observations emerge.

Table 6: Results of the Alternative Design Simulations

Trial	Notes	Surf-Avg Peltier Temp (°C)	Therm. Resist. (K/W)	% Change in Therm. Resist	Volume (cm^3)	% Change in Volume
1	Unmodified	43.5	0.553	--	93.4	--
1b	Split fins (n = 18)	42.9	0.533	-4%	89.0	-4.7%
2b	Split fins without gaps (n = 20)	42.2	0.510	-8%	92.4	-1.0%
3b	Triangular fins (n = 18)	44.4	0.583	5%	83.3	-10.8%
4b	Triangular fins (n = 32)	40.2	0.443	-20%	102.6	9.9%
5b	Gyroid fins	40.7	0.460	-17%	88.7	-5.0%

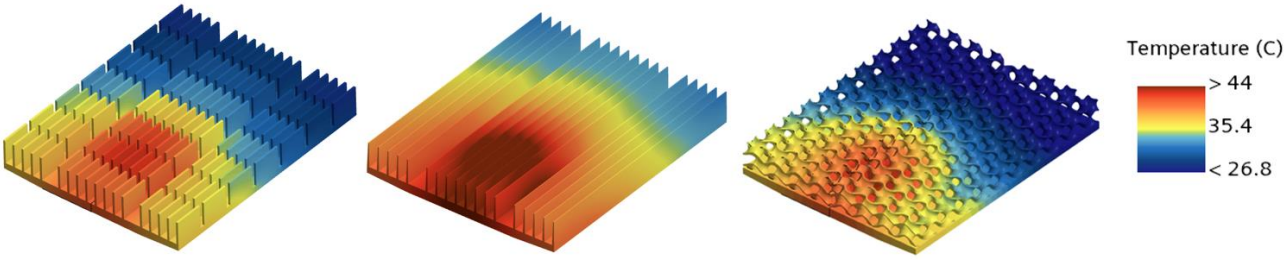

Figure 19: Results of Select Alternative Design Simulations

The split fins slightly reduce thermal resistance. The authors theorize that the gaps in each fin provide additional paths to distribute flow more evenly over the heat sink. The viability of split fins design depends on the cost-benefit analysis, which is discussed in the following section of this report.

Triangular fins become more beneficial as the number of fins increases. At the existing number of fins (n = 18), triangular fins led to a higher thermal resistance in the heat sink. However, in heat sinks with 32 fins, triangular fins outperform the standard rectangular fins (Trial 4b versus Trial 15). The authors attribute the triangular fins' increase in performance with fin count to changes in the effective fin spacing. As was revealed in the parametric study, the existing fin spacing was already optimized. Hence, as more fins are added, the fin spacing becomes smaller than ideal. Triangular fins have the effect of widening the spaces between the fins, allowing more airflow and improving convective heat transfer.

The gyroid heat sink lowered thermal resistance by 17% but was outperformed by the much simpler 32-fin designs. Still, both 32-fin heat sinks increased the volume of material required by 10-32%, while the gyroid fins decreased the material requirements by 5%. The authors also note that the gyroid fins were poorly optimized. The small pore size led to regions of stagnant flow within the lattice, as shown in Figure 20. Increasing the size of the gyroid unit cell could alleviate this issue. Nevertheless, the manufacturing costs of this design are prohibitively high for a cheap mini fridge.

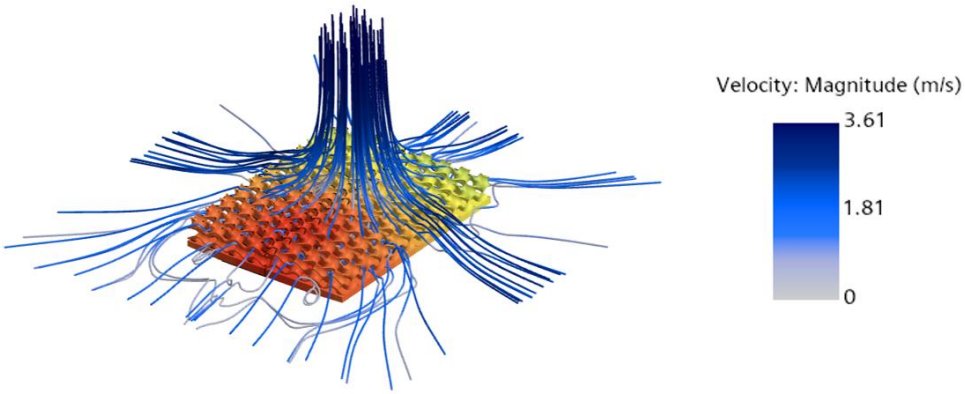

Figure 20: Air Flow Through Gyroid Fins

To compare the results of the CFD simulations as they correlate to COP change, the TEC1-12704 data sheet [8] was used to correlate surface temperatures and heat rates to current flows and voltages, thus allowing for the calculation of power consumption. Once these values were obtained as shown in the Figure 20, the COP was able to be calculated for each heat sink of interest. The results of these findings are summarized in section 4.

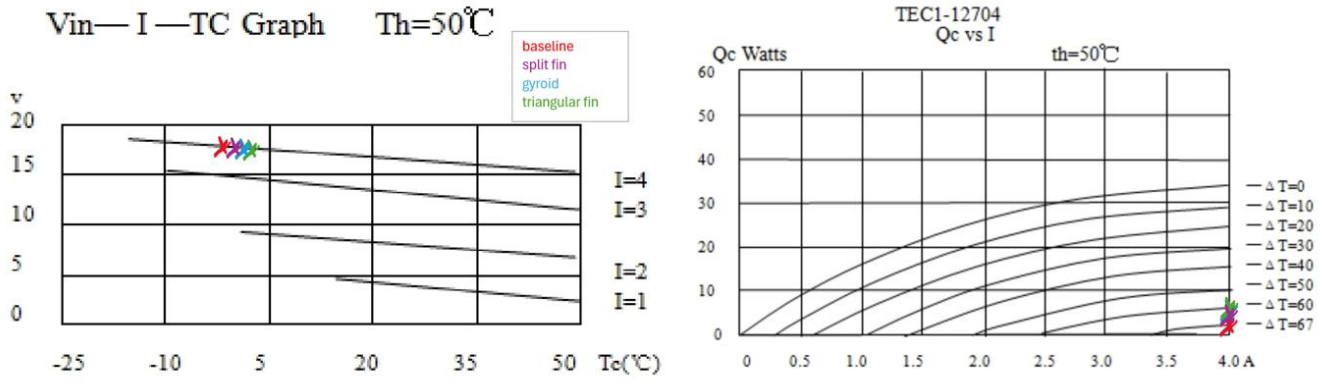

Figure 21: Annotated Data Sheet Figures

4 Budget Report

The analysis of the improvements suggested from a cost basis were conducted as per the methodology section. The results from the heat sink simulations shown in Table 8 are used to compare the geometries of heat sinks that were analyzed with respect to the amount of COP improvement that would result. This follows the method for analyzing COP as discussed above.

Table 8: Results from the Heat Sink Simulations

from checking data sheet:	**Baseline**	**Split Fins (n = 18)**	**Triangular Fins (n = 32)**	**Gyroid**
ΔT	51.5	50.2	48.2	48.7
I (Assume full current draw for cooling)	4	4	4	4
V (from Qc plots)	18	17.75	17	17.5
P_in	72	71	68	70
Qc (from plot)	9	10	13	12
COP	0.125	0.141	0.191	0.171
COP % Change from Baseline	0%	12.8%	53%	37%
Cost % Change	-	6.8%	9.90%	57020.40%
COP : Cost % Change	-	1.88	5.35	0.000651

The triangular fin design with 32 fins yields a COP improvement to Cost % Change ratio of 5.35, which is a quite good value. This is a much stronger design decision compared to a complex additively manufactured design, which adds significant cost. The split fin design also increased COP more than it increased cost, but it is a significantly less-appealing option due to the requirements for machining after the extrusion process. Further analysis should be conducted to investigate future changes of this design to utilize a triangular finned heat sink with a larger number of fins. It would also be possible to create a split-triangular-fin design that combines the best elements of each, but this is left for future work. This is estimated to have a significant improvement on the energy efficiency of the mini fridge. Figure 22 shows the final, optimized heat sink design.

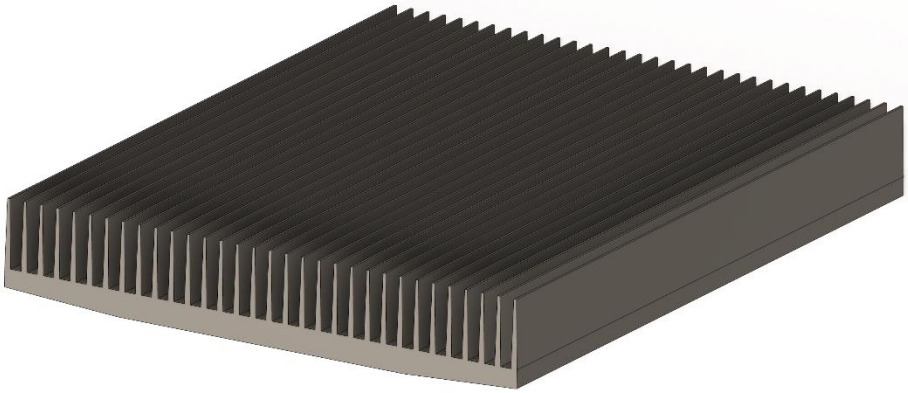

Figure 22: Optimized Heat Sink Design

5 Work Schedule

The work schedule for our project was organized into several key phases, each with specific tasks and deadlines. Below is a summary of the major milestones and progress from the project grant chart shown in Figure 23:

1. **Disassembly of the Fridge (6/17/24 - 6/21/24):**
    - The initial phase involved disassembling the Chefman Iceman Mini Fridge to understand its internal structure and components. This task was completed on schedule.
2. **Progress Presentation (6/11/24 - 6/27/24):**
    - We prepared and delivered a progress presentation, which summarized the initial findings and outlined the next steps for the project. This was completed successfully.

3. **Finalization of Technical Specifications (6/21/24 - 7/8/24):**
    - The development of technical specifications for the components and improvements. This was completed successfully.
4. **Data Collection and Calculations (7/8/24 - 7/14/24):**
    - We gathered data for the fan and performed calculations related to fin efficiency. These tasks were essential for building an accurate model of the fridge and determining simulation conditions.
5. **Modeling and Simulation (7/8/24 - 7/14/24):**
    - The fridge was modeled for simulation, and conditions were determined. This allowed us to assess the performance of the fridge and identify areas for improvement.
6. **Selection and Implementation of Design Improvements (7/1/24 - 7/8/24):**
    - Various design improvements were chosen based on the simulation results. This included optimizing the heat sink design and enhancing the overall thermal management of the system.
7. **New Technical Specifications Estimation (7/8/24 - 7/15/24):**
    - New technical specifications were estimated based on the selected improvements, ensuring that the modifications would meet the desired performance criteria.
8. **Final Presentation (7/12/24 - 7/22/24):**
    - A final presentation was prepared to showcase the project's outcomes, including the improvements made to the fridge’s performance.
9. **Final Report (7/15/24 - 7/29/24):**
    - The project concluded with the submission of a final report, detailing the entire process from disassembly to the implementation of improvements.

The project followed a structured timeline, ensuring that all tasks were completed efficiently and on time. Each phase built upon the previous one, leading to a comprehensive analysis and enhancement of the minifridge's thermal system.

TASK	PROGRESS	START	END
Dissasemble fridge	100%	6/17/24	6/21/24
Progress presentation	100%	6/11/24	6/27/24
Finalize technical specifications	100%	6/21/24	7/8/24
Fan Data	100%	7/8/24	7/11/24
Fin Equations	100%	7/8/24	7/14/24
Model of Fridge for Sim	100%	7/8/24	7/14/24
Simulation Conditions Determined	100%	7/8/24	7/14/24
Select Improvements to Model	100%	7/8/24	7/14/24
Chose design improvments	100%	7/1/24	7/8/24
New tech. spec. estimation	100%	7/8/24	7/15/24
Final presentation	100%	7/12/24	7/22/24
Final report	100%	7/15/24	7/29/24

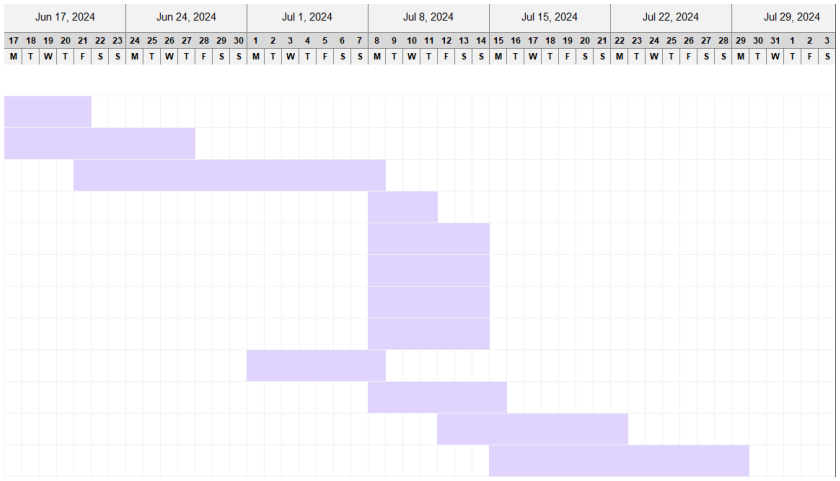

Figure 23: Project Gant Chart

6 Conclusions and Recommendations

This study demonstrates the significant value of using Computational Fluid Dynamics (CFD) tools to optimize the design of thermal systems like the Chefman Iceman Mini Fridge. By leveraging CFD, we were able to directly analyze and enhance the performance of the fridge's cooling system, specifically focusing on the cold side Peltier cooler and the hot side heat sink. Unlike traditional methods that rely heavily on simplified equations and assumptions, CFD provides a more nuanced and accurate representation of fluid flow and heat transfer. This allowed us to identify flow-based improvements that go beyond basic techniques like maximizing surface area, leading to a more efficient and effective thermal management solution. For the hot side, our simulations project the CFD-optimized heat sink will improve the mini fridge's overall COP by up to 53%, with only a small cost increase of 9.9% versus the existing heat sink.

Recommendations:

1. **Mesh Convergence Studies:**
    - To further validate the accuracy of our CFD simulations, it is recommended to perform mesh convergence studies. This ensures that the results are independent of the mesh size and that the simulations provide reliable data for design optimization.
2. **Optimized Gyroid Fin Pattern:**
    - Consider exploring a better-optimized gyroid fin pattern with larger pores. This design could potentially offer improved heat dissipation while maintaining structural integrity, leading to further enhancements in the fridge's performance.
3. **Detailed Cost Analysis:**

- A more comprehensive cost analysis should be conducted. Our current analysis did not account for labor and shipping costs, which are crucial factors in real-world applications. Additionally, our assumption that the cost of all extrusions is directly proportional to the material may not hold true, particularly with the thin fins proposed in the new heat sink design. Manufacturing challenges associated with these finer structures could impact the overall cost and feasibility of the design.

References

[1] “Yate D80SM-12B Loon D80SM-12 with Plug (2500rpm) (80x80x15mm) Air Cooling Axial Fans : Amazon.ca: Electronics.” Accessed: Aug. 04, 2024. [Online]. Available: https://www.amazon.ca/Yate-D80SM-12-Stecker-2500rpm-80x80x15mm/dp/B003ZO662Y

[2] R. Krishnamurthy, “The Importance of Flow Alignment of Mesh,” GridPro Blog. Accessed: Apr. 07, 2024. [Online]. Available: https://blog.gridpro.com/the-importance-of-flow-alignment-of-mesh/

[3] “The Cost of Custom Aluminum Extrusions: 5 Key Factors,” Gabrian International. Accessed: Jul. 25, 2024. [Online]. Available: https://www.gabrian.com/cost-of-custom-aluminum-extrusions/

[4] “Instant Quoting for 3D Printing and CNC Machining,” Xometry. Accessed: Jul. 25, 2024. [Online]. Available: https://www.xometry.com/quoting/home/

[5] V. Kanate, A. Pardeshi, F. Charde, K. Kolase, A. Bhise, and P. Kothmire, “Numerical Investigation on Performance of CPU Heat Sinks,” in *Fluid Mechanics and Fluid Power, Volume 1*, K. M. Singh, S. Dutta, S. Subudhi, and N. K. Singh, Eds., Singapore: Springer Nature, 2024, pp. 361–372. doi: 10.1007/978-981-99-7827-4_29.

[6] L. Wallat, P. Altschuh, M. Reder, B. Nestler, and F. Poehler, “Computational Design and Characterisation of Gyroid Structures with Different Gradient Functions for Porosity Adjustment,” *Materials (Basel)*, vol. 15, no. 10, p. 3730, May 2022, doi: 10.3390/ma15103730.

[7] D. Mahmoud *et al.*, “Enhancement of heat exchanger performance using additive manufacturing of gyroid lattice structures,” *Int J Adv Manuf Technol*, vol. 126, no. 9, pp. 4021–4036, Jun. 2023, doi: 10.1007/s00170-023-11362-9.

[8] “TEC1-12704 Specification.” Hebei I.T. (Shanghai) Co., Lt d. Accessed: Aug. 05, 2024. [Online]. Available: https://peltiermodules.com/peltier.datasheet/TEC1-12704.pdf